

Materials for bulk acoustic wave (BAW) resonators and filters

H.P. Löbl^{a,*}, M. Klee^a, R. Milsom^b, R. Dekker^c, C. Metzmacher^a, W. Brand^a, P. Lok^d

^aPhilips Research Laboratories, Weisshausstr. 2, D-52066 Aachen, Germany

^bPhilips Research Laboratories, Cross Oak Lane, Redhill RH1 5HA, UK

^cPhilips Research Laboratories, Prof. Holstlaan 4, NL-5656 AA Eindhoven, The Netherlands

^dPhilips Discrete Semiconductors, MSI, Gerstweg 2, NL-6534 AE Nijmegen, The Netherlands

Abstract

Thin film bulk acoustic wave (BAW) resonators and filters are appropriate for mobile communication systems operating at high frequencies between 1–10 GHz. The resonance frequency is mainly determined by the thickness of the piezoelectric layer. Piezoelectric films used for this application are, therefore, several 100 nm in thickness (up to approx. 2 μm) depending on frequency. Piezoelectric thin film materials used for bulk acoustic wave devices include AlN, ZnO thin films for small bandwidth applications and also PZT films for wide bandwidth applications. Within Philips piezoelectric AlN and PbZr_xTi_{1-x}O₃ (PZT) layers are investigated with respect to their potential for RF micro-electronic applications. High quality AlN films with strong *c*-axis orientation are achieved by optimum sputter deposition conditions and by applying suited nucleation layers. Electromechanical coupling factors *k* of 0.25±0.03, which are close to the bulk data, have been found in highly *c*-axis oriented AlN thin films. The relationship between sputter deposition conditions, AlN films structure on the one hand and electromechanical coupling factor *k* and relevant electrical parameters on the other hand will be discussed. A one-dimensional physical model is used to describe the bulk acoustic wave resonator's electrical impedance data accurately. Thin PZT films are grown via sol–gel processing. These films show high electro-mechanical coupling factor *k* of 0.3–0.6 and are therefore attractive for wide bandwidth filter applications. © 2001 Elsevier Science Ltd. All rights reserved.

Keywords: Aluminum nitride; Bulk acoustic wave; PZT; Resonators

1. Introduction

For mobile communication applications in the GHz range, small sized band pass filters with low insertion loss and good out of band rejection are required. New concepts for surface acoustic wave filters (SAW) are studied to extend their frequency range. Here especially substrates with high acoustic velocities such as diamond are under investigation.¹ With the strong progress in thin film technologies for complex systems such as AlN or PZT in the last 10 years, also bulk acoustic wave filter (BAW) concepts are gaining more and more importance for the high frequency market,^{10–15} BAW filters operating in the GHz range require thin piezoelectric layers in the order of a few μm (see Fig. 1). An acoustic wave is excited electrically in a thin piezoelectric film. Hereby the fundamental thickness extensional mode is

employed. An acoustic reflector substantially reduces energy loss into the substrate.

Attractive piezo-electric films for BAW resonators and filters are aluminum nitride (AlN),^{2–4} ZnO¹⁵ and PbZr_xTi_{1-x}O₃ (PZT).⁵ In this paper we focus on AlN and PZT films. With AlN films an electro-mechanical coupling coefficient *k_t* of approx. 0.25 and low losses can be achieved, if strongly *c*-axis oriented AlN films are grown. AlN is, therefore, an excellent material for small bandwidth filters (bandwidth < 5%), as can be derived from the relation between resonance *f_r* and anti-resonance frequency *f_a* and the coupling coefficient *k* [see Eq. (1)].⁸ The achievable bandwidth is determined by the difference of *f_a*–*f_r* and thus by the value of *k* (see Fig. 2).

$$k = \frac{\pi}{2} \cdot \sqrt{\left(\frac{f_a - f_r}{f_a}\right)} \quad (1)$$

PbZr_xTi_{1-x}O₃ ceramics are very well known piezo-electric as well as ferro-electric materials. They show,

* Corresponding author. Tel.: +49-241-600-3597; fax: +49-241-600-3465.

E-mail address: hans-peter.loebel@philips.com (H.P. Löbl).

dependent on the composition and doping after poling, electro-mechanical coupling coefficients of as high as 0.7. Making these materials available by means of thin film technology, RF filters with bandwidth $> 5\%$ can be offered. In this paper we report on deposition and growth of AlN and PZT films and their potential for BAW resonator/filter applications.

2. Experimental

AlN films were deposited by pulsed reactive d.c. magnetron sputtering in a BAK 600 deposition system pumped with a cryo-pump. A pulse frequency of 20 kHz was used to avoid arcing.

The AlN films were deposited onto Si wafers coated with a (111) oriented Pt electrode. As adhesion layer a thin titanium film was applied. Alternatively Si wafers coated with thermally grown SiO₂ and Si wafers with native oxide were used as substrates to study the film growth. The AlN films were characterized by X-ray diffraction $\theta/2\theta$ scans (Philips Fine Focus PW2213/20) and

by measuring the rocking curve of the (0002) AlN peak to determine the tilt of the lattice planes in the (0002) oriented columnar grains. TEM cross-sections were made to determine the film morphology and grain structure (TEM: Philips CM12). The film surface was investigated by atomic force microscopy (Topometrix Explorer TMX2000). The thickness of the films was determined by using a profilometer (type: Sloan Dektak 3030).

Non-doped PbZr_xTi_{1-x}O₃ thin films as well as lanthanum doped PZT films are grown by means of modified sol-gel processing⁶ on Si (100) with a Ti/Pt electrode. Films with a thickness of 0.5–1.5 μm are deposited by several spin-on steps and are fired after each spin on at 600 °C. The layers receive a final anneal in oxygen at 650 °C. The top-metallization was deposited by sputtering and lithographically patterned to achieve series type resonators. The growth of the thin films was characterized with respect to phase formation and grain size by means of X-ray diffraction analysis and SEM. BAW resonators were made on 4" and 6" wafers using different acoustic reflectors.

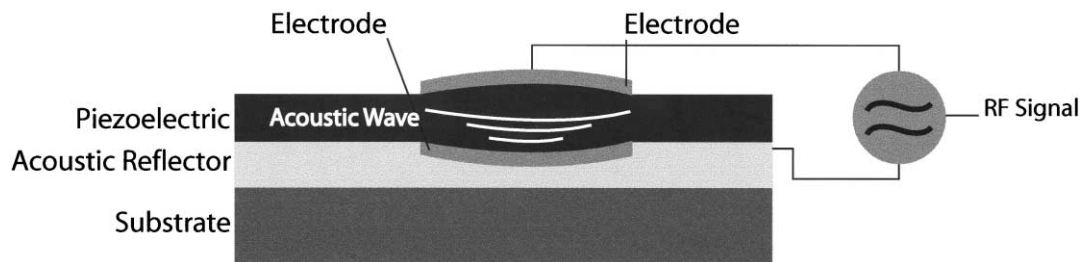


Fig. 1. BAW resonator: principle of operation A longitudinal standing acoustic wave is excited electrically in a thin piezoelectric film. The layer thickness of the piezoelectric film and of the electrodes determines the resonance frequency of the BAW resonator.

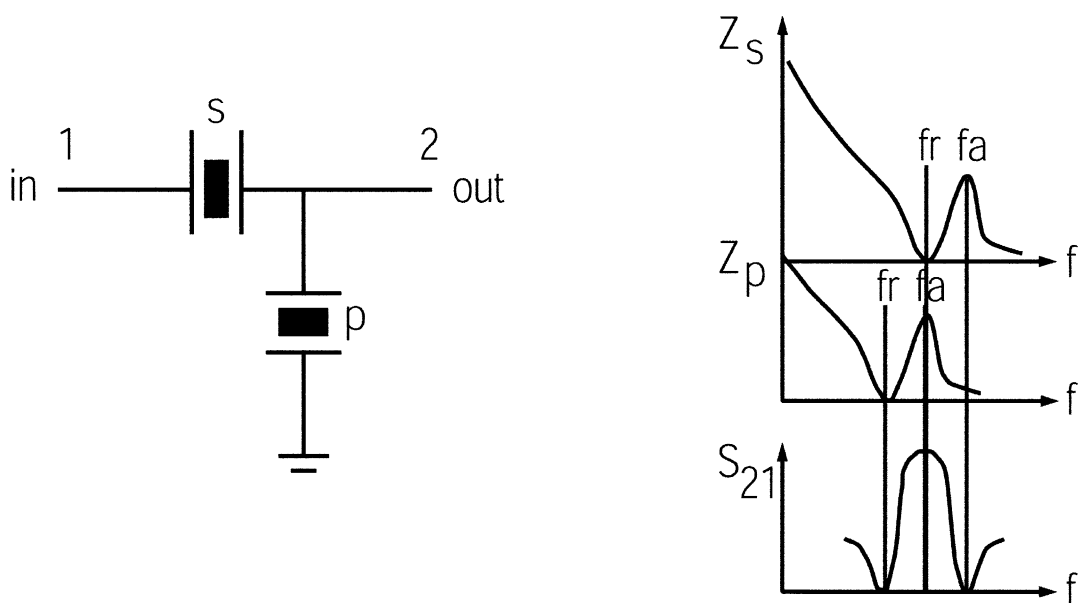


Fig. 2. BAW filter principle: the electrical impedance curve of the parallel resonator p is shifted in frequency relative to the series resonator s by $\Delta f = f_a - f_r$. This creates a band-pass filter characteristics in S_{21} .

The electrical impedance of the piezoelectric films was determined from S11 parameter measurements using a wafer microprobe. These measurements were done with an 8510C HP network-analyzer. For some of the films the electrical impedance was measured with a HP4291A RF-impedance analyzer. The data for k were extracted from the determination of f_a [maximum of resistance $\text{Re}(Z)$] and f_r [maximum of conductance $\text{Re}(Y)$] using Eq. (1).

3. Results and discussion

3.1. AlN films

To achieve high piezo-electric coupling to the required thickness extensional mode in AlN layers, they have to be grown oriented in (0002) direction. Therefore, columnar AlN grains with the c -axis perpendicular to the substrate are needed. The texture of sputtered AlN films depends on the sputter deposition conditions, on the substrate surface (nucleation layer), and on deposition temperature. Also the AlN layer thickness has an influence on the quality and orientation of the grains. The effect of substrate temperature for AlN films grown on a SiO₂ surface (thermal oxide on silicon) and a Pt (111) surface is shown in Fig. 3. It can be seen clearly that elevated temperatures improve the (0002) orientation of the AlN films which goes along with an increase of the electromechanical coupling coefficient k_t . For a deposition temperature of 450 °C we found a k_t of 0.13, at 550 °C k_t was 0.25, and at 650 °C k_t was found to be 0.28.

The growth of the AlN films and their (0002) orientation are strongly affected by the various types of substrates: on Pt (111) the AlN orientation has the best quality (see Figs. 3–5) due to the fact that the hexagonal AlN structure (lattice constant $a = 0.311$ nm) matches well with the Pt (111) plane.¹⁶ On Pt (111) the size of the

crystallites in the columns is in the order of the film thickness, as can be deduced from XRD and TEM measurements. The AlN grains are growing quasi epitaxial on Pt. The epitaxial growth is supported by temperature (Fig. 3). Therefore, the c -axis orientation of AlN on Pt surfaces is improved by increasing temperature.

For BAW devices it is important to get smooth interfaces and surfaces for all the individual layers of the resonators. Therefore, we investigated the roughness of AlN films grown on different substrates by AFM. The surface roughness of AlN films is influenced by the surface roughness of the substrate as can be seen from Fig. 6. Especially on tungsten electrodes with their high surface roughness the growing AlN layer (thickness approx. 3.5 μm, deposition temperature 650 °C) shows a similar roughness, which means that the ad -atoms of the growing AlN layer do not have sufficient energy to move across the rough W surface. On thermal SiO₂, glass and Pt surfaces, which are quite smooth, the ad -atoms of the growing AlN layer have sufficient energy and the surface roughness of the AlN films is determined by the growth mechanism of the AlN layer itself.

The sputtering pressure has also some effect on orientation. The c -axis orientation of the AlN films is decreased as the pressure is increased from 2.4×10^{-3} mbar to 4.9×10^{-3} mbar. This is mainly due to the reduced energy of particles impinging on the substrate at higher sputtering pressures caused by scattering in the gas phase. Therefore, deposition has to be conducted at low pressures. Sputtering at low pressure is also recommended to reduce the tensile stress in the AlN films. In our BAK600 deposition system sputtering of AlN films was performed statically with a $17'' \times 5''$ target on $4''$ wafers. Under these conditions the wafers show a big horizontal variation in layer thickness of approx. $\pm 10\%$. One can expect that the angle of incidence of the sputtered atoms is small only for the wafer's center. The AlN columns therefore grow vertical on the substrate (Fig. 4) only at the wafer's center. The width of

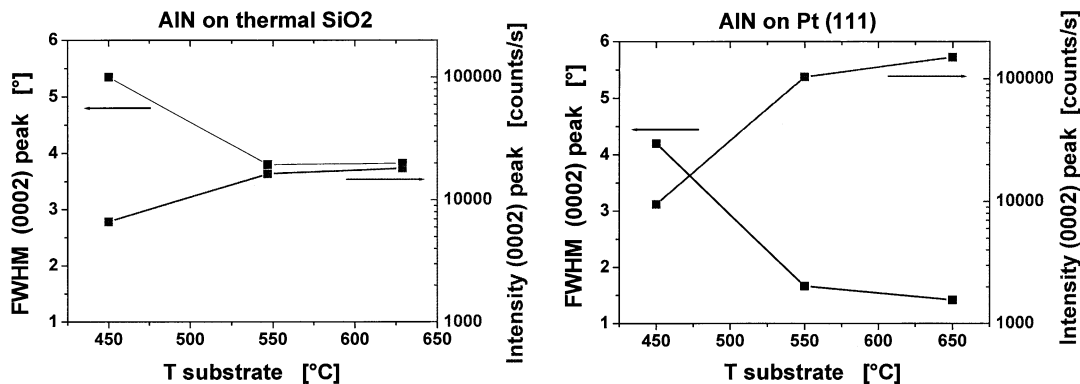


Fig. 3. Orientation of AlN (0002) planes versus substrate temperature as determined by rocking curve measurements of the (0002) peak (FWHM). The substrate was Si coated with 500 nm thermal SiO₂ (left) or coated with a 140 nm thick Pt film, which had (111) orientation. The films deposited on Pt(111) at 650 °C had the highest k_t values. Sputter-conditions are kept constant (power 2.6 kW, Ar/N₂ gas ratio 0.28, pressure 1.6×10^{-3} mbar). Layer thickness is 1.4 μm.

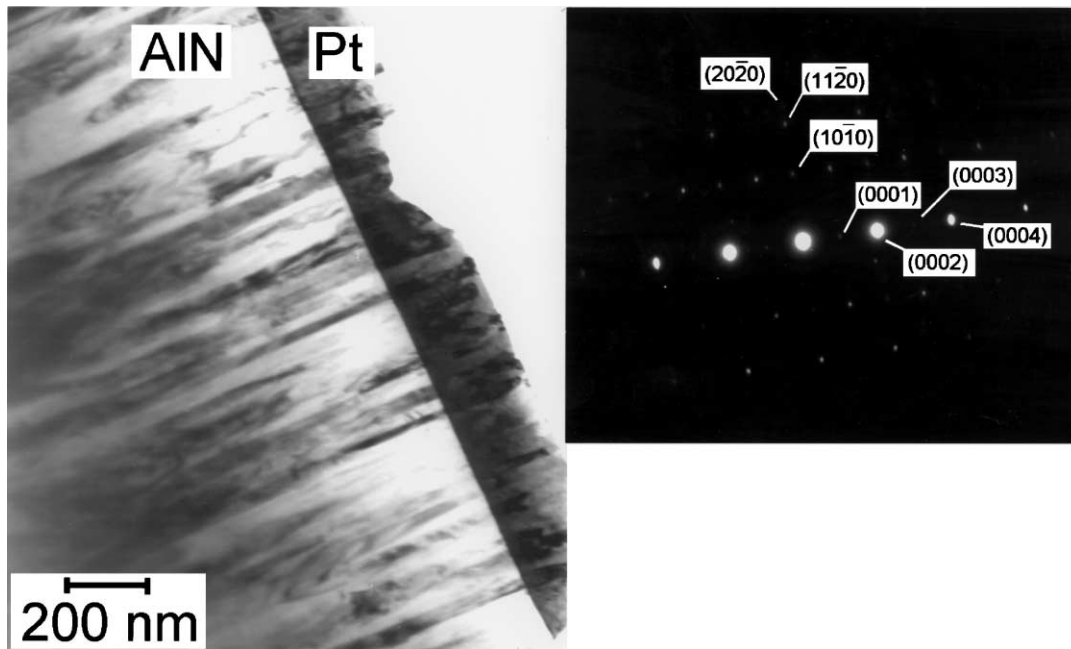


Fig. 4. Growth of *c*-axis oriented AlN films on Pt (111) electrodes: quasi-epitaxial growth on the Pt grains. FWHM of rocking curve of (0002) peak: 1.2°. Sample from center of 4" wafer.

the AlN rocking curve of the (0002) peak is 1.2°, the maximum is at 18° ($2\theta = 36^\circ$) which means that the (0002) lattice planes are not tilted. On a corner of the wafer, however, the angle of incidence is high and the AlN columns grow under an angle of approx. 27° (Fig. 7). The width of the rocking curve of the AlN (0002) peak is 5° if the rocking curve is measured in the direction of the gradient of the layer thickness distribution. The maximum of the rocking curve is shifted by 3°, which means that the (0002) lattice planes are tilted by this angle. Thus, the tilt of the grains (27°) is much lar-

ger than the tilt of the (0002) lattice planes, which is only 3°. High-resolution TEM investigations and the selected area diffraction pattern in Fig. 7 also confirm this result.

In Fig. 7 the growth mechanism at large angle of incidence can be seen very clearly. AlN starts growing quasi epitaxial on the Pt (111) surface. The tilt of the crystals is almost zero in the nucleation phase. When a certain thickness is reached (100–200 nm) the crystals bend due to shadowing effects until they are inclined by 27° which is approximately the angle of incidence.

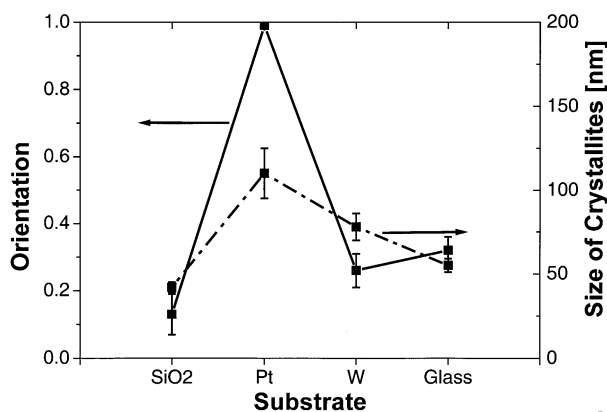


Fig. 5. Influence of substrate surface on (0002) orientation and crystallite size (coherence length perpendicular to substrate surface) of AlN layers. (0002) Orientation is defined as: area of (0002) peak/ Σ area of all peaks (1.0 means 100% *c*-axis orientation). Substrate temperature 640 °C, film thickness approx. 3.5 μm , power 2.6 kW, Ar/N₂ gas ratio 0.43. Substrates used were SiO₂ (500 nm thermally grown oxide on Si), a Pt (111) electrode on Si, a tungsten electrode on Si, and Corning AF45 glass.

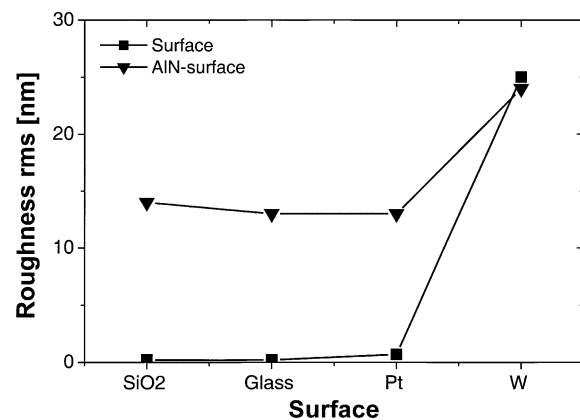


Fig. 6. Surface roughness of different nucleation layers and of the AlN layers deposited on top of these layers. AlN film thickness was 3.5 μm , the deposition temperature 645 °C, power 2.6 kW, Ar/N₂ gas ratio 0.43, pressure 2×10^{-3} mbar. Substrates used were SiO₂ (500 nm thermally grown oxide on Si), a Pt (111) electrode on Si, a W electrode on Si and Corning AF45 glass.

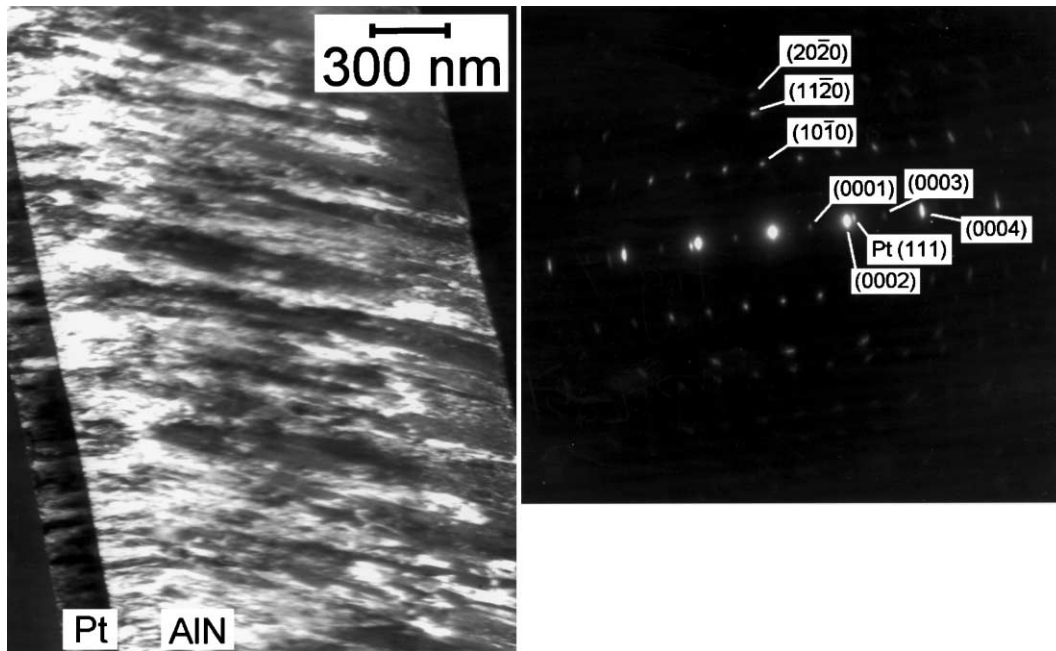


Fig. 7. Growth of *c*-axis oriented AlN films on a Pt (111) electrode. Sample from corner of wafer (layer thickness in center of wafer approx. 2 μm , at corner of wafer approx. 1.8 μm). Angle of incidence of sputtered atoms: 27°. Tilt of (0002) lattice planes: 3°. FWHM of rocking curve of (0002) peak: 5°.

However, the lattice planes become only slightly tilted 3°. This growth mechanism is schematically illustrated in Fig. 8.

This is a very important result, since we expect that the electromechanical coupling coefficient k should not be influenced strongly by this small tilt of the lattice planes. When we determine k on different positions on the wafer we find indeed that the variation over the wafer is weak despite the large variations in angle of incidence of the sputtered species (see Fig. 9). On the abscissa of Fig. 9 the tilt of the AlN (0002) lattice plane as derived from the maximum of the rocking curves is shown. The rocking curve FWHM width is 1.2° for the sample from the wafer center and is broader for samples which show a large tilt of the (0002) lattice plane (1.5° and 5°, respectively).

To realize high Q BAW resonators and filters one has not only to deposit high quality piezoelectric layers, but also to avoid loss of acoustic energy from the resonators. This can be achieved by an acoustic reflector which can consist of several $\lambda/4$ layers of high and low acoustic impedance.^{10–12,17} An alternative is a simple reflector consisting of one thin layer of very low acoustic impedance. We used e.g. a reflector made of a SiO₂ ceramic with low acoustic impedance. The resonators on this wafer were series type resonators and consisted of a *c*-axis oriented piezoelectric AlN layer sandwiched between two Pt electrodes. The electrical measurement results can be seen below in Fig. 10. Q -factors between 120–150 are determined. The electromechanical coupling coefficient k was 0.24, which is close to the bulk

value given in literature. The FWHM of the rocking curve, as determined for the (0002) AlN peak, is 1.8°. The electrical impedance curves were simulated using the one-dimensional theory of Nowotny and Benes.⁹ For the simulation we used a dielectric constant of 10 for the AlN layer and a k_t of 0.25. The longitudinal velocity of sound was assumed to be 11.000 m/s and for the AlN density we assumed 3.3 g/cm³. A parasitic inductance of 0.4 nH was added to explain the electrical impedance data [Im(Z)]. The sheet resistance of the resonator leads and a calibration offset accounts for the difference between simulated and measured Re(Z).

From this data we conclude that a reflector made of ceramic SiO₂ can be used and offers a quality factor of approx. 130–150 and can still be improved by a more careful resonator design. To optimise resonators and filters in a next step the following key elements have to be selected carefully: resonator design, electrode material, and reflector material.

3.2. $\text{PbZr}_x\text{Ti}_{1-x}\text{O}_3$ films

High quality piezoelectric thin films for broad-band RF applications have been studied in the system $\text{PbZr}_x\text{Ti}_{1-x}\text{O}_3$.¹⁸ Films have been grown by means of modified sol-gel processing in the system $\text{PbZr}_x\text{Ti}_{1-x}\text{O}_3$ with $0.1 < x < 0.53$. Films with various Zr/Ti ratios have been processed. For selected compositions also lanthanum in the order of 1% up to 5% was doped into the PZT films. As shown in a previous paper,⁶ lanthanum can be homogeneously incorporated from 1% up

to 15% into the PZT lattice. The $\text{PbZr}_x\text{Ti}_{1-x}\text{O}_3$ as well as lanthanum doped $\text{Pb}_{1-1.5y}\text{La}_y\text{Zr}_x\text{Ti}_{1-x}\text{O}_3$ films with $x = 0.1-0.35$ and $y = 0.01-0.02$ grow with a tetragonal distortion on top of Pt (111) electrodes. For $\text{PbZr}_{0.35}\text{Ti}_{0.65}\text{O}_3$ films fired at 600°C and finally annealed at 650°C , a tetragonal distortion of the perovskite lattice with $a = b = 0.4008$ (2) nm and $c = 0.4113$ (3) nm was found. Under these processing conditions, the films are fine grained and show a columnar morphology.⁷ The columnar morphology has not only been determined for thin films of $0.2-0.5\ \mu\text{m}$ but also for thick films of $1-1.5\ \mu\text{m}$. The c/a ratio of these fine-grained films is with 1.026 slightly smaller than reported for bulk ceramics ($c/a = 1.037$). All the layers investigated here grow on Pt (111) oriented electrodes with a (100) and (111) orientation. (001) Peaks are also present, but weaker in intensity.

BAW resonator devices were processed with tetragonal $\text{PbZr}_x\text{Ti}_{1-x}\text{O}_3$ ferroelectric thin films. With a PZT thickness of approx. $1.3\ \mu\text{m}$ (composition: $\text{Pb}_{1.1}\text{Zr}_{0.35}\text{Ti}_{0.65}\text{O}_3$) the resonance frequency was 0.9 GHz, for a

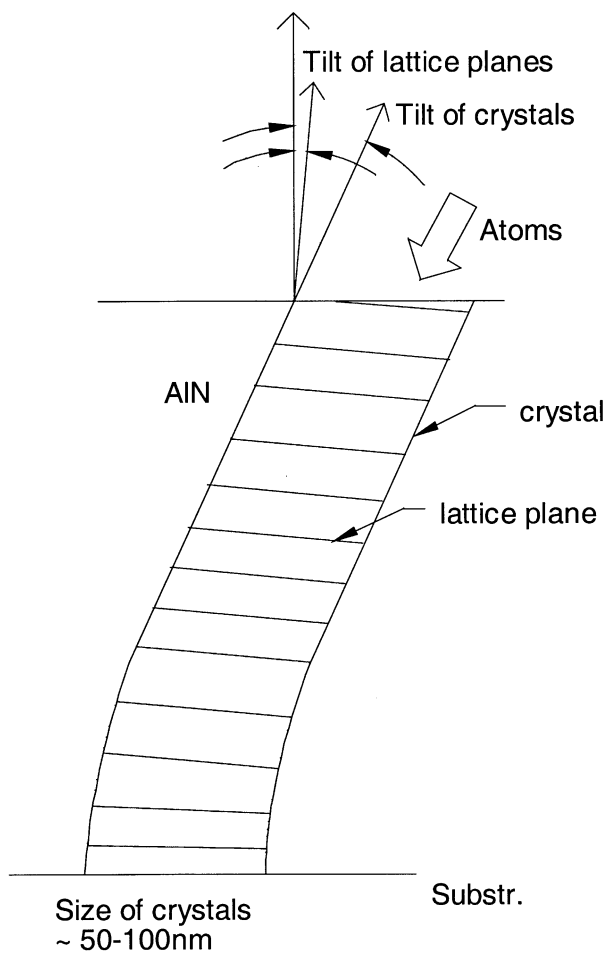


Fig. 8. Schematic visualization of AlN growth when angle of incidence is not zero. The crystallites are more tilted than the lattice planes.

PZT thickness of approx. $0.5\ \mu\text{m}$ (composition: $\text{Pb}_{1.1}\text{Zr}_{0.35}\text{Ti}_{0.65}\text{O}_3$) the resonance frequency of the BAW resonators was 2.3 GHz. Acoustic reflectors of ceramic SiO_2 for the resonators operating at 0.9 GHz or alternatively a multi-layer reflector consisting of $\lambda/4$ layers with high and low acoustic impedance for the resonators operating at 2.3 GHz were applied.

Poling experiments were performed on series resonators to increase the coupling coefficient k_t . The series resonators were poled at temperatures between RT and 150°C for typically 10 min and cooled down in an electric field of $100\ \text{kV/cm}$ up to $300\ \text{kV/cm}$. The electrical impedance of BAW resonators, measured with a network analyzer, is shown in Fig. 11. The poling procedure increased the coupling factor k_t up to values between 0.28 and 0.5. For the resonator operating at 0.9 GHz a Q value of 67 can be achieved making use of a single layer acoustic reflector. For the 2.3 GHz resonator a Q value of 18 could be reached (see Fig. 11). To our knowledge, this is the first time that Q values are reported for PZT thin film BAW resonator devices. The

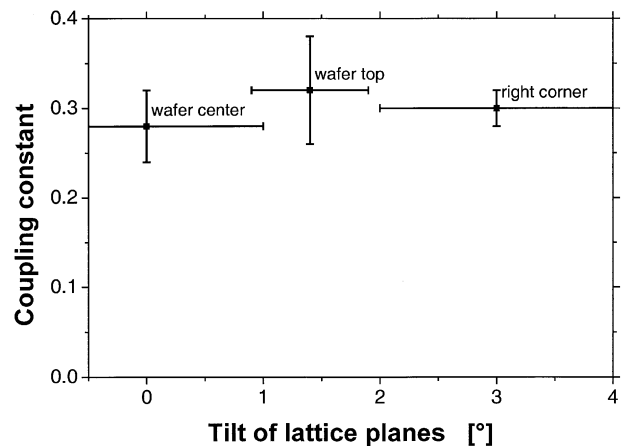


Fig. 9. Variation of electromechanical coupling constant k with position on wafer, which is correlated with the tilt of (0002) plane.

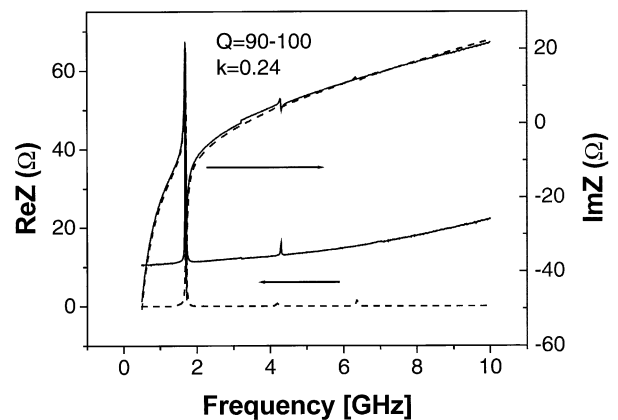


Fig. 10. BAW resonator measurement (full line) and simulation (dashed line): real and imaginary part of the electrical impedance Z . A ceramic SiO_2 layer with low acoustic impedance was used for the reflector.

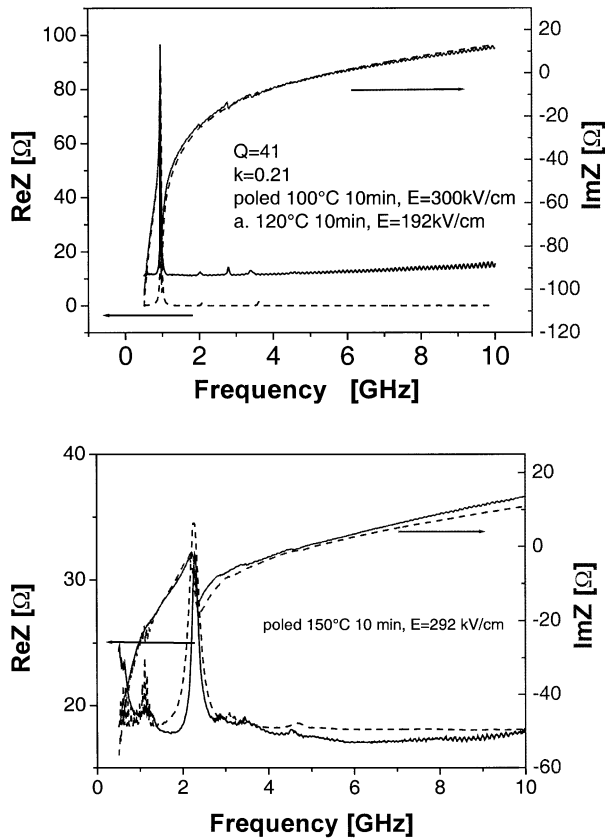


Fig. 11. BAW resonator with PZT (composition: $\text{Pb}_{1.1}\text{Zr}_{0.35}\text{Ti}_{0.65}\text{O}_3$): measurement (full line) and simulation (dashed line) of electrical impedance Z . Wafer with ceramic SiO_2 layer used for the reflector (top) and with multi-layer reflector (bottom). A quality factor of up to 67 can be reached on the ceramic reflector (resonance frequency at approx. 0.9 GHz, PZT thickness 1.3 μm), on the multi-layer reflector a Q factor of 18 has been determined (resonance frequency at approx. 2.3 GHz, PZT thickness 0.5 μm). The electromechanical coupling factor k_t can be as high as 0.5 depending on poling conditions.

one dimensional model of Nowotny and Benes⁹ which we use for simulation gives a good description of the electrical impedance data of the resonators (see Fig. 11), if we introduce high acoustic losses into the resonator. Dielectric losses, in contrast, cannot explain the electrical impedance data consistently.

Whether these acoustic losses are material losses in the PZT itself, or caused by scattering of the acoustic wave or by geometrical effects such as insufficient energy trapping due to the low aspect ratio (aspect ratio = resonator size/resonator thickness) of the PZT resonators, is under investigation.

4. Conclusions

Piezo-electric AlN films with strong c -axis orientation can be made with high rate d.c. magnetron sputter deposition. k Values of up to 0.25 ± 0.03 have been

found. These films are attractive for small bandwidth RF applications. BAW resonators have been demonstrated making use of a single layer ceramic SiO_2 acoustic reflector. Device Q factors of 130–150 have been achieved. For wide bandwidth applications non-doped as well as lanthanum doped $\text{PbZr}_x\text{Ti}_{1-x}\text{O}_3$ thin films were investigated. Piezoelectric coupling coefficients up to 0.5 have been measured.

Acknowledgements

We would like to thank our colleagues H.D. Bausen, B. Krafczyk, T. Michielsen, G. Much and O. Wunnicke at the Philips Research Laboratories Aachen and Eindhoven. This work is supported by the European Commission within the Project 'Microwave Electro-acoustic Devices for Mobile and Land based Applications (MEDCOM, IST-1999-11411)'.

References

- Nahkahata, H. and Kitabayashi, H., Study on surface acoustic wave characteristics of SiO_2 /interdigital transducer/ ZnO /diamond structure and fabrication of 2.5 GHz narrow band filter. *Jpn. J. Appl. Phys.*, 1998, **37**, 2918.
- Naik, R. S., Reif, R., Lutsky, J. S. and Sodni, C. G., Low temperature deposition of highly textured aluminum nitride by direct current magnetron sputtering for application in thin film resonators. *J. Electrochem. Soc.*, 1999, **146**, 691.
- Dubois, M. A. and Mural, P., Properties of aluminum nitride thin films for piezoelectric transducers and microwave filter applications. *Appl. Phys. Lett.*, 1999, **74**, 3023.
- Dubois, M. A., Mural, P., Matsumoto, H. and Plessky, V., Solidly mounted resonator based on aluminum nitride thin film. *1998 IEEE Ultrasonics Symposium*, 1998, p. 909.
- Hsueh, C. C., Tamagawa, T., Ye, C., Helegeson, A. and Polla, D. L., Sol gel derived ferroelectric films in silicon micromachining. *Integrated Ferroelectrics*, 1993, **3**, 21.
- Klee, M., Mackens, U., Kiewitt, R., Greuel, G. and Metzmacher, C., Ferroelectric thin films for integrated passive components. *Philips J. of Research*, 1998, **51**, 363–387.
- Klee, M., Mackens, U. and De Veirman, A., $\text{Pb}(\text{Zr}_x\text{Ti}_{1-x})\text{O}_3$ films produced by modified sol gel technique: thin film growth and electrical properties. *Ferroelectrics*, 1993, **141**, 211–218.
- IEEE Standard on Piezoelectricity. American Institute of Standards, Std. 176-1987.
- Nowotny, H. and Benes, E., General one-dimensional treatment of the layered piezoelectric resonator with two electrodes. *J. Acoust. Soc. Am.*, 1987, **82**, 513.
- Lakin, K. M., Kline, G. R. and McCarron, K. T., High Q microwave acoustic resonators and filters. *IEEE Transactions on Microwave Theory and Techniques*, 1993, **41**, 2139.
- Lakin, K. M., Kline, G. R. and McCarron, K. T., Development of miniature filters for wireless applications. *IEEE Transactions on Microwave Theory and Techniques*, 1995, **43**, 2933.
- Lakin, K. M., Thin film resonators and filters. *1999 IEEE Ultrasonics Symposium, Lake Tahoe*, 1999, p. 895.
- Larson III, J. D., Ruby, R., Bradley, P. and Oshmyansky, Y., A BAW antenna duplexer for the 1900 MHz PCS band. *IEEE Ultrasonics Symposium, Lake Tahoe*, 1999, p. 887.

14. Dubois, M. A., Muralt, P. and Plesky, Y., BAW resonator based on AlN thin films. *1999 IEEE Ultrasonics Symposium, Lake Tahoe*, 1999, p. 907.
15. Osbond, P., Beck, C. M., Brierley, C. J., Cox, M. R., Marsh, S.P. and Shorrock, N. M., Influence of ZnO and electrode thickness on the performance of thin film bulk acoustic wave resonators. *1999 IEEE Ultrasonics Symposium, Lake Tahoe*, 1999, p. 911.
16. Zhang, W., Vargas, R., Goto, T., Someno, Y. and Hirari, T., Preparation of epitaxial AlN films by electron cyclotron resonance plasma assisted chemical vapour deposition on Ir- and Pt-coated sapphire substrates. *Appl. Phys. Lett.*, 1994, **64**, 1359.
17. Newell, W. E., Face mounted piezoelectric resonators. In Proc. IEEE, 1965, **53**, 575.
18. Löbl, H. P., Klee, M., Wunnicke, O., Kiewitt, R., Dekker, R. and Pelt, E., Piezoelectric AlN and PZT films for micro-electronic applications. *1999 IEEE Ultrasonics Symposium, Lake Tahoe*, 1999, p. 1031.